Electronic Supplementary Material (ESI) for Journal of Materials Chemistry C.

Supporting Information

Manipulating Room-temperature Phosphorescence via Lone-pair Electrons and Empty-orbital Arrangements and Hydrogen Bonds Adjusting

Haodong Sun, Zongliang Xie, Hailan Wang, Wazhang Wu, Beibei Du, Cao Guan, Tao Yu**

1 Synthesis and Characterization of Compounds

4-Bromobenzophenone, 2-Bromobenzophenone were purchased from Energy-Chemical and were used directly without any further purification. Bis(pinacolato)diboron, potassium acetate (CH_3COOK), dioxane, 2-methyltetrahydrofuran (2-Me-THF), and [1,1'-bis(diphenylphosphino)-ferrocene]dichloropalladium ($Pd(dppf)Cl_2$) were purchased from Sigma-Aldrich. The other reagents were purchased from Aladdin Industrial. The details of the synthetic procedures for the final compounds were listed in the following part. Final compounds were characterized by ^1H NMR, high performance liquid chromatography (HPLC)and high resolution EI mass spectrometry.

Synthetic Routes

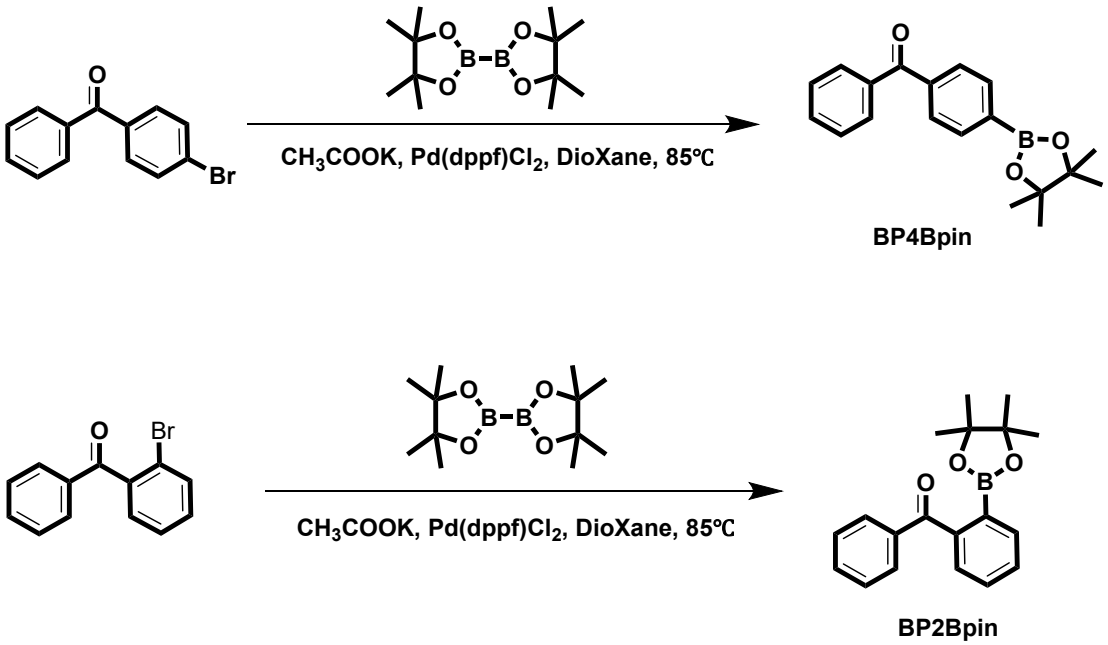

Scheme S1 Synthetic routes for compounds BP4Bpin and BP2Bpin.

Synthetic Details

Phenyl(4-(4,4,5,5-tetramethyl-1,3,2-dioxaborolan-2-yl)phenyl)methanone (BP4Bpin)

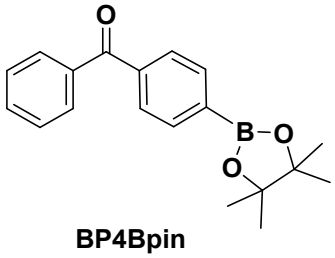

BP4Bpin

4-Bromobenzophenone (2.00 g, 7.66 mmol), Bis(pinacolato)diboron (3.89 g, 15.32 mmol), potassium acetate (2.63 g, 26.81 mmol), Pd(dppf)Cl_2 (5 %), and recently opened dioxane (40 mL) were mixed in a dried 250 mL flask under argon atmosphere. After refluxing for 24 hours, the reaction mixture was cooled to room temperature. The organic solvent was distilled out, and the residual solid was dissolved in dichloromethane (DCM) and washed with water. After removal of the solvents, the crude products were purified through silica-gel chromatography with n-hexane/ Ethylacetate (8/1, v/v) to give BP4Bpin as a white powder (1.58 g, yield: 66.9%). ^{1}H NMR (500 MHz, $CDCl_3$, 298 K), (TMS, ppm): δ = 7.92 (d, J = 8.19 Hz, 2H), 7.76-7.80 (m, 4H), 7.57-7.61 (m, 1H), 7.46-7.49 (t, 2H), 1.37 (s, 12H). ^{13}C NMR (500 MHz, $CDCl_3$, 298 K), (ppm): 24.90, 84.21, 128.30, 129.02, 130.13, 132.53, 135.57, 137.53, 139.79, 196.93. High Resolution EI-MS: m/z found: 308.1579 [M]+; cald for [C19H21BO3]: 308.1584.

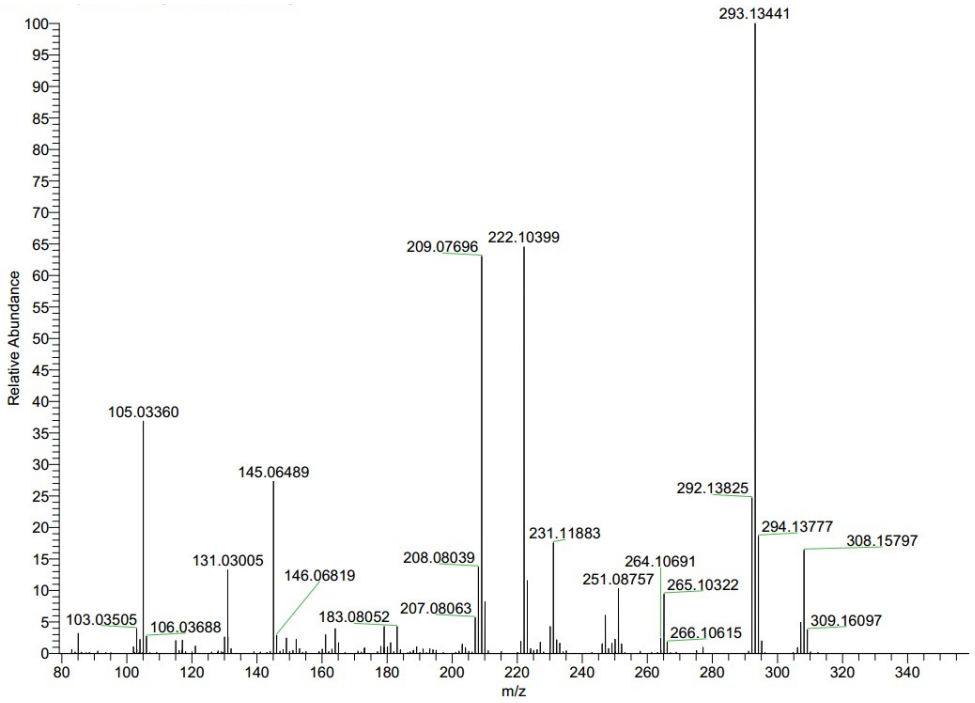

Figure S1 High Resolution EI mass spectrum of BP4Bpin.

Phenyl(2-(4,4,5,5-tetramethyl-1,3,2-dioxaborolan-2-yl)phenyl)methanone (BP2Bpin)

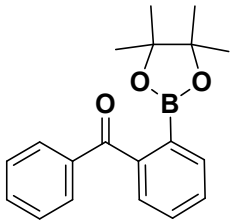

BP2Bpin

BP2Bpin were synthesized according to the similar experimental procedures of BP4Bpin. A white powder was achieved. Yield: 1.58 g, yield: 66.9%. ^{1}H NMR (500 MHz, $CDCl_3$, 298 K), (TMS, ppm): δ = 7.78 (d, J = 8.37 Hz, 2H), 7.74 (d, J = 7.39 Hz, 2H), 7.50-7.56 (m, 3H), 7.46-7.49 (m, 1H), 7.42-7.45 (t, 2H), 1.18 (s, 12H). ^{13}C NMR (126 MHz, $CDCl_3$, 298 K), (ppm): 198.17, 143.67, 138.16, 133.82, 132.39, 130.33, 130.03, 129.71, 128.92, 128.21, 84.01, 83.51, 25.04, 24.56. High Resolution EI-MS: m/z found: 309.1656 [M]+; cald for [C19H21BO3 + H^+]: 309.1584.

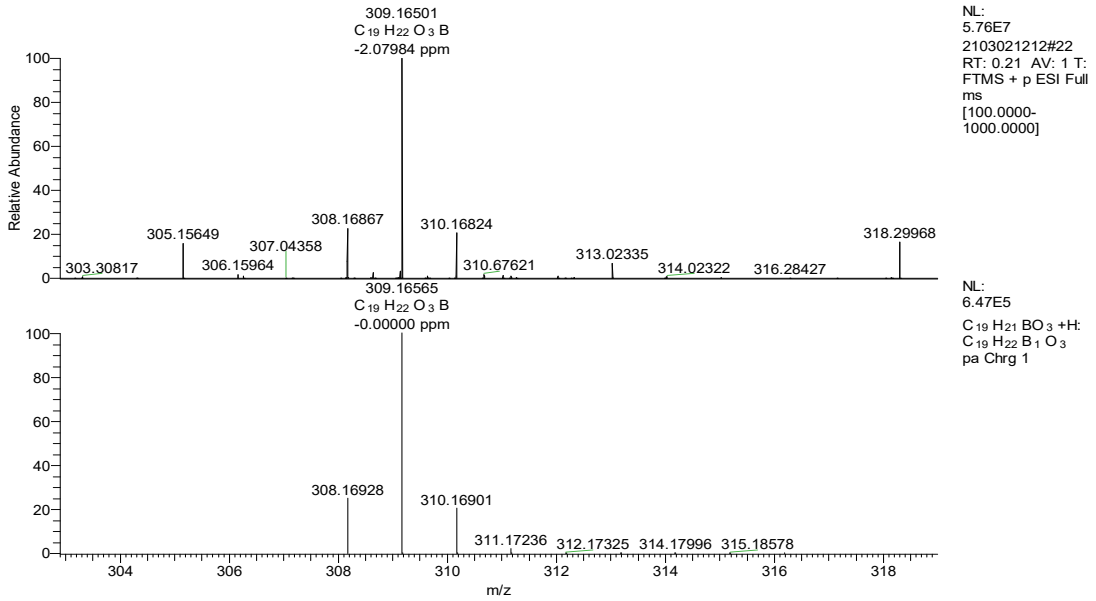

Figure S2 High Resolution ESI mass spectrum of BP2Bpin.

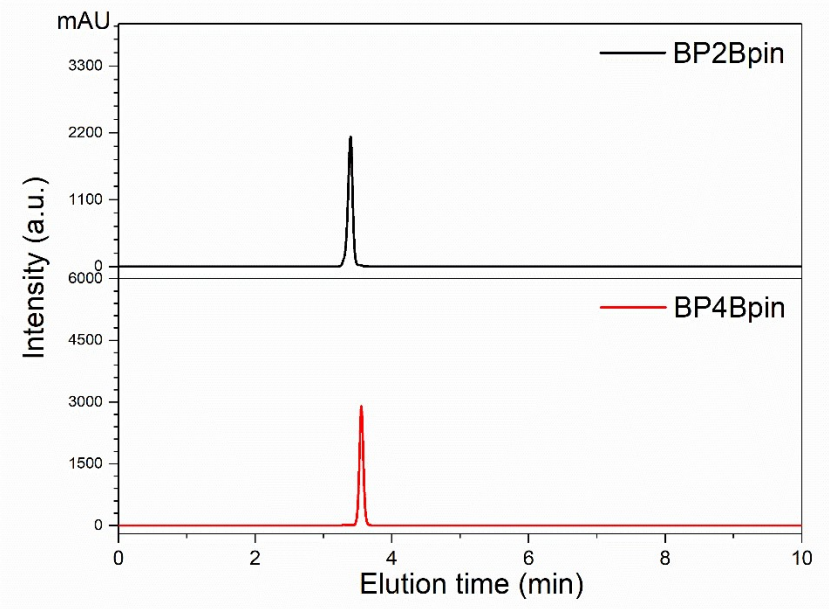

Figure S3 HPLC diagrams of BP2Bpin and BP4Bpin.

2 Physical measurements and instrumentations

^{1}H NMR spectra were performed with on a Bruker AVANCE NEO 500 Nuclear Magnetic Resonance Spectrometer ((500 MHz)) in $CDCl_3$ using tetramethylsilane (TMS) as the internal standard. High Resolution EI mass spectra were collected from a MAT95XP-HRM spectrometer.

High performance liquid chromatography (HPLC) was performed on an UltiMate 3000. The UV-visible absorption spectra of solutions were performed on Hitachi U-3900. The steady emission and afterglow emission were measured by a Shimadzu RF-5301 PC spectrometer or an Ocean Optics Maya Pro2000 with 310 nm and 365nm Rhinospectrum RhinoLED as the excitation source. Fluorescence and phosphorescence decay curves were tested on a Hamamatsu compact fluorescence lifetime spectrometer (FLS-1000). Wide-angle XRD measurements were performed at 298 K using an X-ray diffractometer (Bruker, D8 Advance). Variable temperature test system was built by ourselves. Single-crystal ananlyses of *n*-BP4Bpin, *c*-BP4Bpin and BP2Bpin were determined using Bruker D8 Quest X-ray Single Crystal Diffractometer with a (Cu) X-ray source.

3 Theoretical calculations

Molecular geometries were extracted in single crystals and performed by Gaussian 09W program package with time-dependent density functional theory (TD-DFT) with Beck's three-parameter hybrid exchange functional [1] and Lee, and Yang and Parr correlation functional [2] (B3LYP) with 6-311G* basic set. Natural transition orbital (NTO) analysis was extracted based on TD-DFT results and visualized via Gaussview (6.0.16). Spin-orbital couplings (SOC) matrix elements were calculated via ORCA (program vision 4.2.1) based on B3LYP/G 6-311G*. Non-covalent interactions (NCI) of intramolecular and intermolecular interactions analyses were carried out by Multiwfn[3] with reduced density gradient (RDG) and independent gradient model (IGM), respectively.[4, 5] Electrostatic potential (ESP) analysis on the basis of the single crystal geometry were performed with the Multiwfn 3.7. The ESP and NCI results were rendered via Visual Molecular Dynamics (VMD) software (version 1.9.3).[6]

Single-crystal data of BP2Bpin, *n*-BP4Bpin and *c*-BP4Bpin

Single-crystal data of BP2Bpin, *n*-BP4Bpin and *c*-BP4Bpin were collected by a Bruker D8 Quest X-ray Single Crystal Diffractometer with a (Cu) X-ray source. The single-crystal structures were solved by Olex2 (program vision 1.3) and expanded using Fourier techniques. All non-H atoms of the compounds were refined with anisotropic thermal parameters. The hydrogen atoms were added in idealized positions and refined with fixed geometry according to their carrier atoms. CCDC numbers of the single-crystal structure of BP2Bpin, *n*-BP4Bpin and *c*-BP4Bpin are 2071524, 2071525 and 2071526, respectively.

Crystal data for BP2Bpin: $C_{19}H_{21}BO_3$ (M = 308.17 g/mol), monoclinic, space group $P2_1/c$, a = 8.6701(3) Å, b = 9.2394(3) Å, c = 21.0354(6) Å, α=90°, β = 101.4810(10) °, γ=90°, V = 1651.36(9) $Å^3$, Z = 4, T = 275(6) K, μ(CuKα) = 1.54178 mm^{-1}, ρ_c = 1.240 g/cm^3, Reflections collected 18436, Independent reflections 3336 unique [R_{int} = 0.0248, R_{sigma} = 0.0177]. R_1 = 0.0379 (I > 2σ(I)) and wR_2 = 0.1019 (all data). GOF = 1.036.

Crystal data for *n*-BP4Bpin: $C_{19}H_{21}BO_3$ (M = 308.17 g/mol), monoclinic, space group $P2_1/n$, a = 6.20100(10) Å, b = 10.5943(2) Å, c = 25.4359(5) Å, α=90°, β = 92.0660(10) °, γ=90°, V = 1669.93(5) $Å^3$, Z = 4, T = 150.0 K, μ(CuKα) = 1.54178 mm^{-1}, ρ_c = 1.226 g/cm^3, Reflections collected 23678, Independent reflections 3399 unique [R_{int} = 0.1178, R_{sigma} = 0.0467]. R_1 = 0.0403 (I > 2σ(I)) and wR_2 = 0.1076 (all data). GOF = 1.049.

Crystal data for *c*-BP4Bpin: $C_{19}H_{21}BO_3$ (M = 308.17 g/mol), monoclinic, space group $P2_1/c$, a = 12.3412(3) Å, b = 11.8434(3) Å, c = 12.7459(3) Å, α=90°, β = 112.491(2) °, γ=90°, V = 1721.27(8) $Å^3$, Z = 4, T = 150.0 K, μ(CuKα) = 1.54178 mm^{-1}, ρ_c = 1.189 g/cm^3, Reflections collected 15000, Independent reflections 3496 unique [R_{int} = 0.0301, R_{sigma} = 0.0223]. R_1 = 0.0705 (I > 2σ(I)) and wR_2 = 0.1957 (all data). GOF = 1.081.

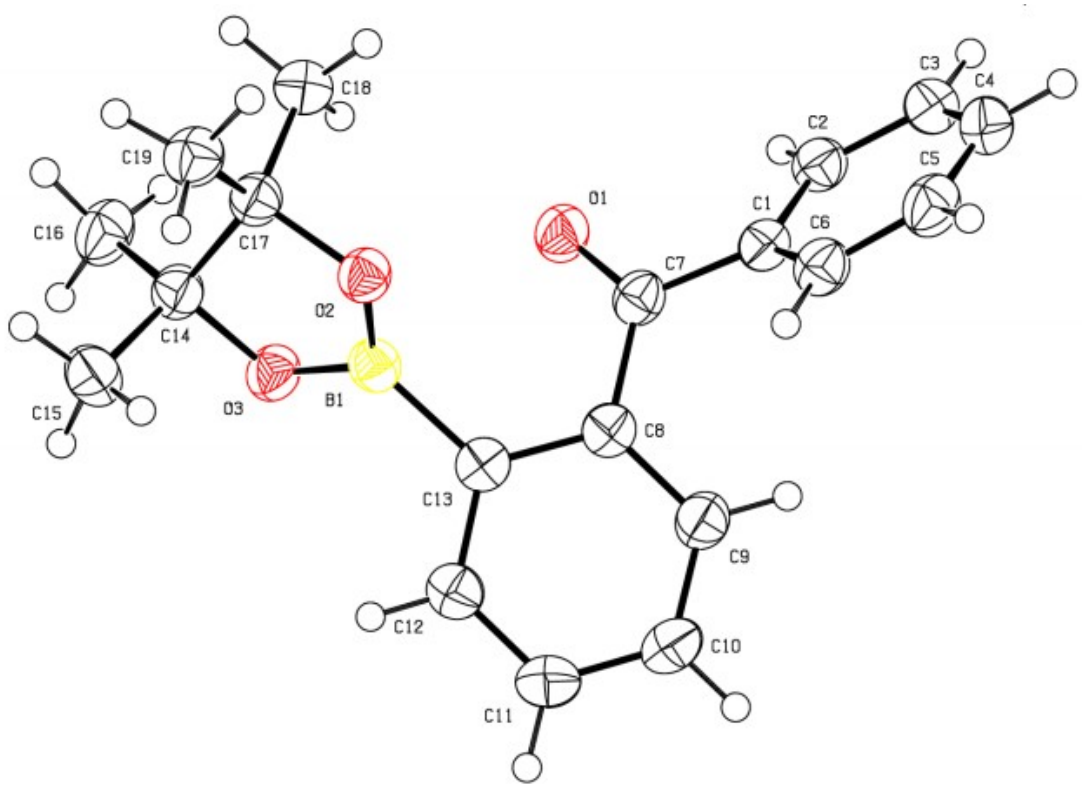

Figure S4 Single crystal structure for BP2Bpin.

Table S1 Bond distance (Å) for BP2Bpin

Atom	Atom	Length/Å	Atom	Atom	Length/Å
O2	C17	1.4630(13)	C2	C3	1.3878(17)
O2	B1	1.3673(15)	C17	C19	1.5169(16)
O3	C14	1.4660(13)	C17	C14	1.5587(16)
O3	B1	1.3663(15)	C17	C18	1.5226(16)
O1	C7	1.2237(13)	C11	C12	1.3893(17)
C13	C8	1.4053(16)	C11	C10	1.3840(18)
C13	C12	1.3954(16)	C9	C10	1.3856(18)
C13	B1	1.5726(16)	C6	C5	1.3845(18)
C1	C7	1.4941(16)	C14	C16	1.5137(17)
C1	C2	1.3925(16)	C14	C15	1.5202(17)
C1	C6	1.3949(16)	C3	C4	1.3855(19)
C8	C7	1.4908(15)	C5	C4	1.3868(19)
C8	C9	1.3931(16)			

Table S2. Bond Angles for BP2Bpin

Atom	Atom	Atom	Angle/°	Atom	Atom	Atom	Angle/°
B1	O2	C17	106.87(9)	C19	C17	C18	110.38(10)
B1	O3	C14	106.65(9)	C18	C17	C14	113.28(10)
C8	C13	B1	122.34(10)	C10	C11	C12	119.67(11)
C12	C13	C8	117.78(10)	C11	C12	C13	121.62(11)
C12	C13	B1	119.88(10)	C10	C9	C8	120.17(11)
C2	C1	C7	118.26(10)	C5	C6	C1	119.89(11)
C2	C1	C6	119.74(11)	O3	C14	C17	102.42(8)
C6	C1	C7	121.84(10)	O3	C14	C16	108.29(9)
C13	C8	C7	118.28(10)	O3	C14	C15	106.50(9)
C9	C8	C13	120.66(10)	C16	C14	C17	115.02(10)
C9	C8	C7	120.44(10)	C16	C14	C15	110.63(10)
O1	C7	C1	119.83(10)	C15	C14	C17	113.18(10)
O1	C7	C8	119.76(10)	C4	C3	C2	120.29(11)
C8	C7	C1	120.38(9)	C11	C10	C9	120.08(11)
C3	C2	C1	119.86(11)	C6	C5	C4	120.32(12)
O2	C17	C19	108.52(9)	C3	C4	C5	119.85(11)
O2	C17	C14	101.96(8)	O2	B1	C13	123.51(10)
O2	C17	C18	107.04(9)	O3	B1	O2	113.65(10)
C19	C17	C14	114.93(9)	O3	B1	C13	122.25(10)

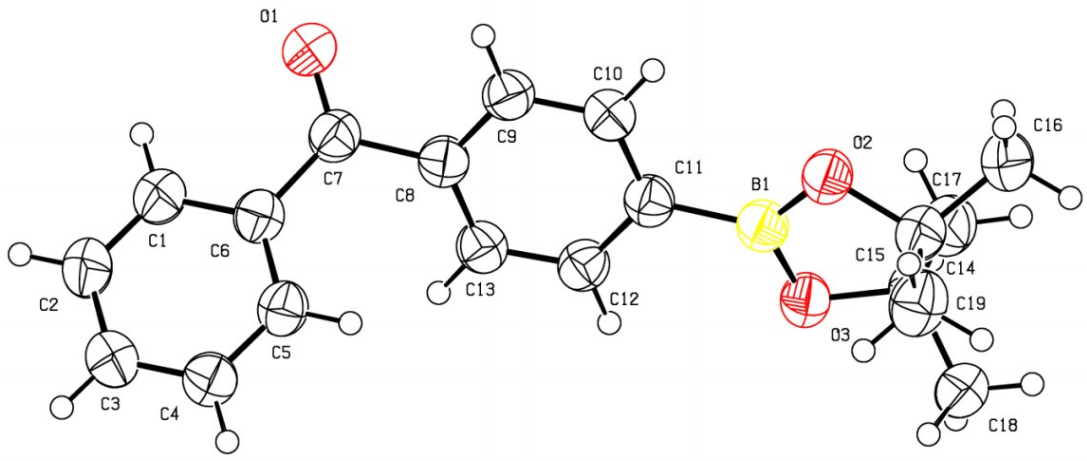

Figure S5 Single crystal structure for *n*-BP4Bpin.

Table S3 Bond distance (Å) for *n*-BP4Bpin

Atom	Atom	Length/Å	Atom	Atom	Length/Å
O2	C15	1.4640(13)	C12	C11	1.4029(16)
O2	B1	1.3666(16)	C12	C13	1.3858(16)
O3	B1	1.3626(16)	C8	C13	1.3963(16)
O3	C14	1.4665(13)	C11	B1	1.5591(16)
O1	C7	1.2209(15)	C6	C1	1.3948(16)
C5	C4	1.3858(17)	C17	C15	1.5216(17)
C5	C6	1.3931(17)	C3	C2	1.386(2)
C9	C10	1.3850(16)	C16	C15	1.5178(16)
C9	C8	1.3998(15)	C15	C14	1.5535(17)
C4	C3	1.3756(18)	C2	C1	1.3841(19)
C7	C8	1.4983(15)	C14	C19	1.5201(19)
C7	C6	1.4943(17)	C14	C18	1.5190(18)
C10	C11	1.3997(16)			

Table S4. Bond Angles for *n*-BP4Bpin

Atom	**Atom**	**Atom**	**Angle/°**	**Atom**	**Atom**	**Atom**	**Angle/°**
B1	O2	C15	106.10(9)	C12	C13	C8	120.37(10)
B1	O3	C14	106.33(9)	C4	C3	C2	119.57(12)
C4	C5	C6	121.00(11)	O2	C15	C17	106.46(10)
C10	C9	C8	119.80(10)	O2	C15	C16	109.00(10)
C3	C4	C5	120.02(11)	O2	C15	C14	102.25(9)
O1	C7	C8	119.47(11)	C17	C15	C14	113.41(11)
O1	C7	C6	120.64(11)	C16	C15	C17	110.44(11)
C6	C7	C8	119.87(10)	C16	C15	C14	114.56(11)
C9	C10	C11	121.52(10)	C1	C2	C3	120.84(12)
C13	C12	C11	120.92(11)	C2	C1	C6	119.97(12)
C9	C8	C7	122.37(10)	O2	B1	C11	122.69(11)
C13	C8	C9	119.36(10)	O3	B1	O2	114.14(10)
C13	C8	C7	118.25(10)	O3	B1	C11	123.16(11)
C10	C11	C12	118.01(10)	O3	C14	C15	102.06(9)
C10	C11	B1	120.28(10)	O3	C14	C19	106.43(10)
C12	C11	B1	121.70(10)	O3	C14	C18	108.82(10)
C5	C6	C7	122.27(10)	C19	C14	C15	113.61(11)
C5	C6	C1	118.60(11)	C18	C14	C15	115.14(11)
C1	C6	C7	119.03(11)	C18	C14	C19	110.03(12)

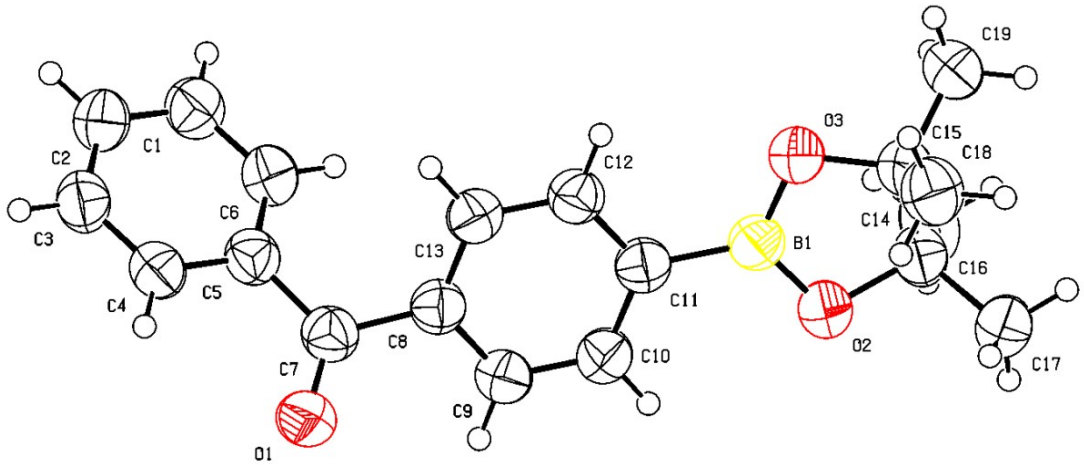

Figure S6 Single crystal structure for *c*-BP4Bpin.

Table S5 Bond distance (Å) for *c*-BP4Bpin

Atom	**Atom**	**Length/Å**	**Atom**	**Atom**	**Length/Å**
O3	C15	1.463(2)	C8	C9	1.394(3)
O3	B1	1.356(3)	C8	C7	1.501(2)
O2	B1	1.366(2)	C7	C5	1.491(3)
O2	C14	1.466(2)	C5	C6	1.393(3)
O1	C7	1.220(2)	C3	C2	1.387(3)
C11	C10	1.402(3)	C6	C1	1.381(3)
C11	C12	1.398(3)	C15	C19	1.516(3)
C11	B1	1.560(3)	C15	C18	1.518(3)
C10	C9	1.384(3)	C15	C14	1.560(3)
C13	C12	1.388(3)	C1	C2	1.386(3)
C13	C8	1.391(3)	C16	C14	1.514(3)
C4	C5	1.400(3)	C17	C14	1.514(3)
C4	C3	1.380(3)			

Table S6. Bond Angles for *c*-BP4Bpin

Atom	**Atom**	**Atom**	**Angle/°**	**Atom**	**Atom**	**Atom**	**Angle/°**
B1	O3	C15	107.36(15)	C4	C3	C2	120.22(18)
B1	O2	C14	106.76(14)	C1	C6	C5	120.09(18)
C10	C11	B1	121.29(16)	O3	C15	C19	108.82(16)
C12	C11	C10	118.01(16)	O3	C15	C18	105.86(17)
C12	C11	B1	120.70(16)	O3	C15	C14	102.28(14)
C9	C10	C11	121.07(17)	C19	C15	C18	109.74(19)
C12	C13	C8	120.20(17)	C19	C15	C14	115.5(2)
C13	C12	C11	121.09(17)	C18	C15	C14	113.82(18)
C3	C4	C5	119.99(18)	C6	C1	C2	120.21(19)
C13	C8	C9	119.40(16)	C1	C2	C3	120.01(19)
C13	C8	C7	122.13(16)	O3	B1	O2	113.92(16)
C9	C8	C7	118.43(16)	O3	B1	C11	123.26(18)
C10	C9	C8	120.22(17)	O2	B1	C11	122.82(17)
O1	C7	C8	119.82(17)	O2	C14	C15	102.42(15)
O1	C7	C5	120.55(17)	O2	C14	C16	105.83(16)
C5	C7	C8	119.63(15)	O2	C14	C17	108.93(16)
C4	C5	C7	118.46(17)	C16	C14	C15	113.19(19)
C6	C5	C4	119.46(17)	C17	C14	C15	114.61(17)
C6	C5	C7	122.00(16)	C17	C14	C16	111.0(2)

Photophysical data and spectra

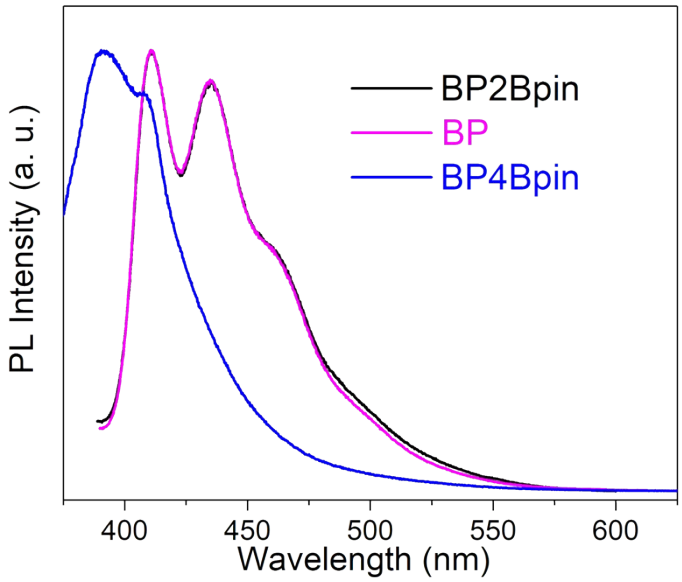

Figure S7 Fluorescence spectra (λ_{ex} = 365 nm) of BP, BP2Bpin and BP4Bpin in DCM solution (1.0×10^{-5} M).

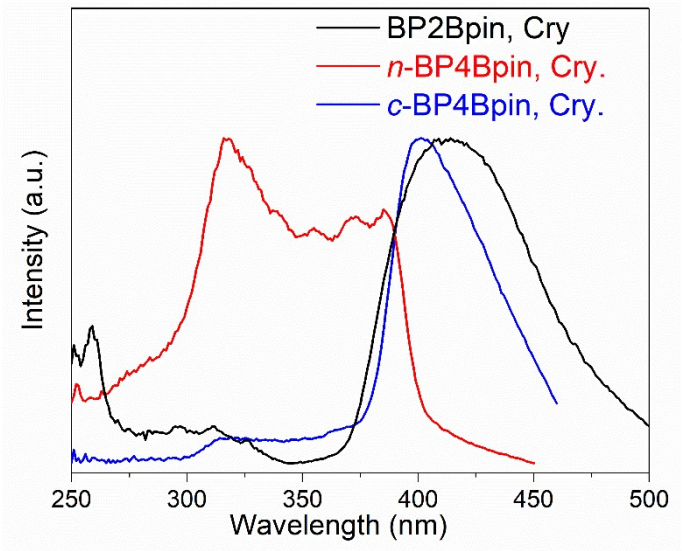

Figure S8 Normalized excitation spectra of crystalline BP2Bpin (λ_{em}= 512 nm), *n*-BP4Bpin (λ_{em}= 490 nm), and *c*-BP4Bpin (λ_{em}= 490 nm).

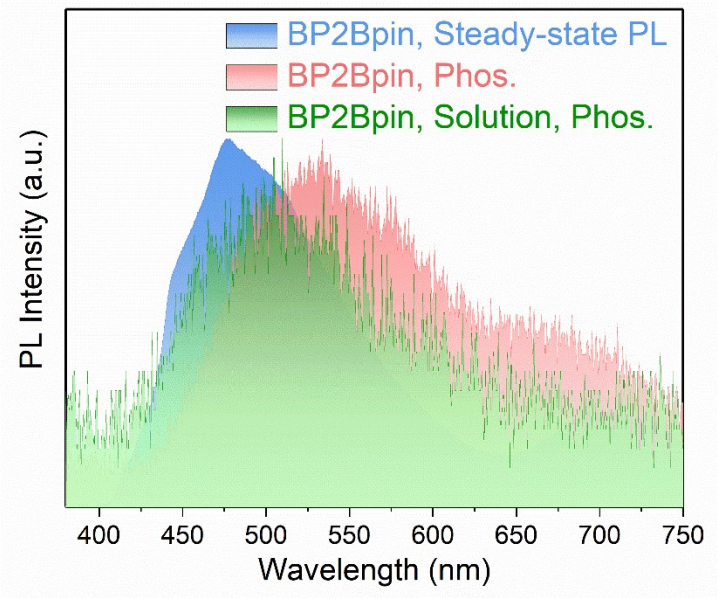

Figure S9 Steady-state PL (blue) and delayed spectra (red) of crystalline BP2Bpin at 77 K, and phosphorescence spectrum (green) of BP2Bpin in 2-MeTHF solution (1.0×10^{-5} M) at 77 K.

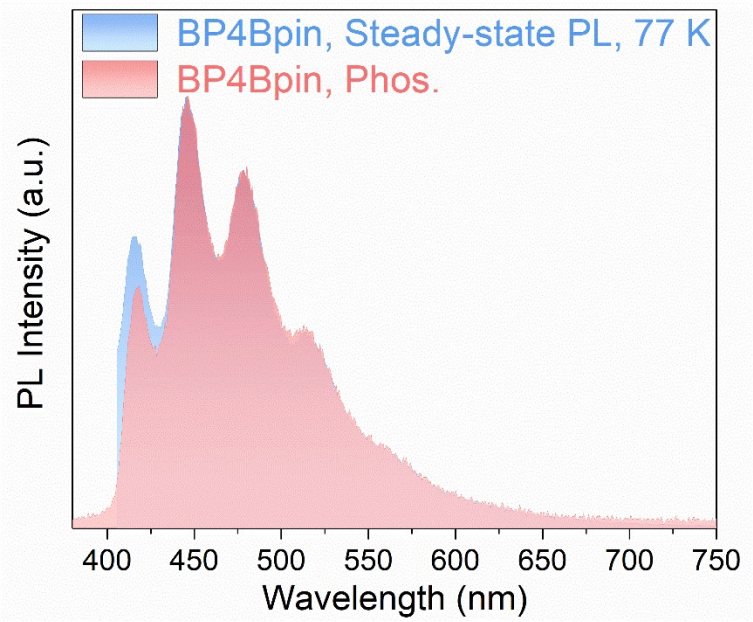

Figure S10 Steady-state PL (blue, λ_{ex} = 365 nm) and delayed spectra (red, delay 8 ms) of BP4Bpin in 2-MeTHF solution (1.0×10^{-5} M) at 77 K.

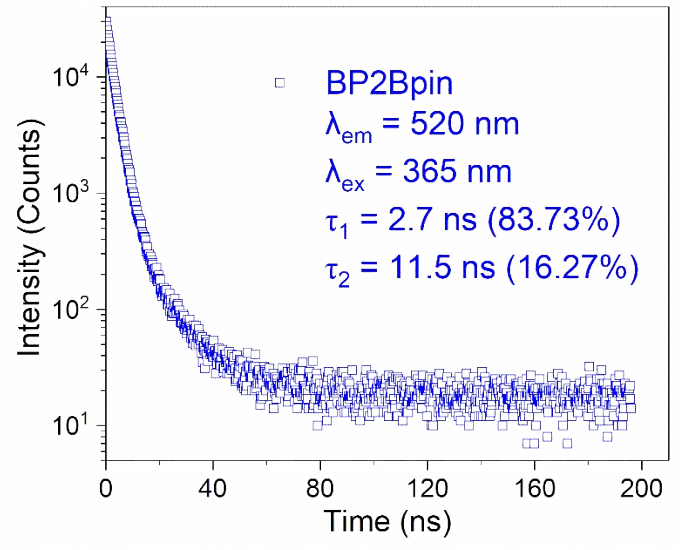

Figure S11 Time-resolved decay curves of crystalline BP2Bpin under 365 nm excitation at 300 K.

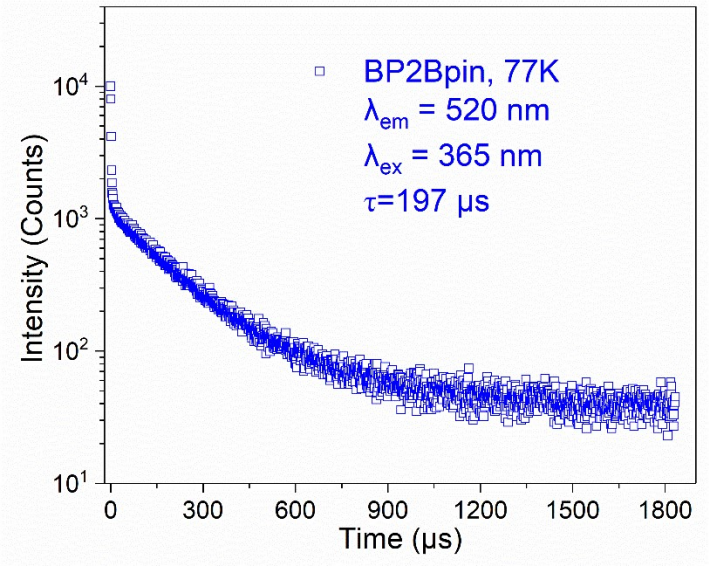

Figure S12 Time-resolved decay curves of crystalline BP2Bpin under 365 nm excitation at 77 K.

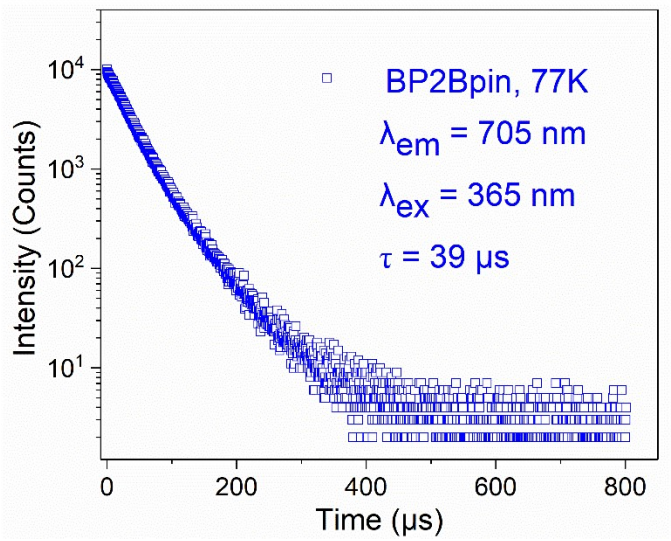

Figure S13 Time-resolved decay curves of crystalline BP2Bpin under 365 nm excitation at 77 K.

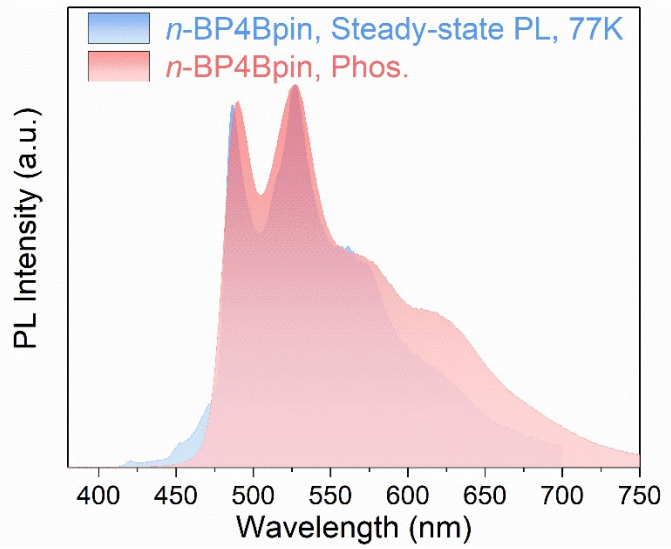

Figure S14 Steady-state PL (blue, λ_{ex} = 365 nm) and delayed spectra (red, delay 8 ms) of crystalline *n*-BP4Bpin at 77 K.

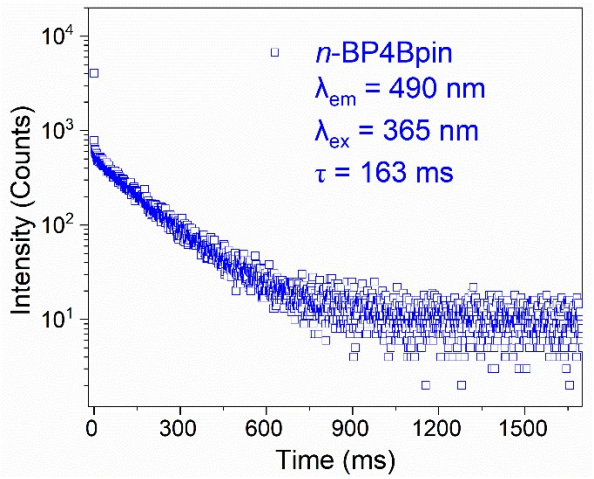

Figure S15 Time-resolved decay curves of crystalline *n*-BP4Bpin under 365 nm excitation at 77 K.

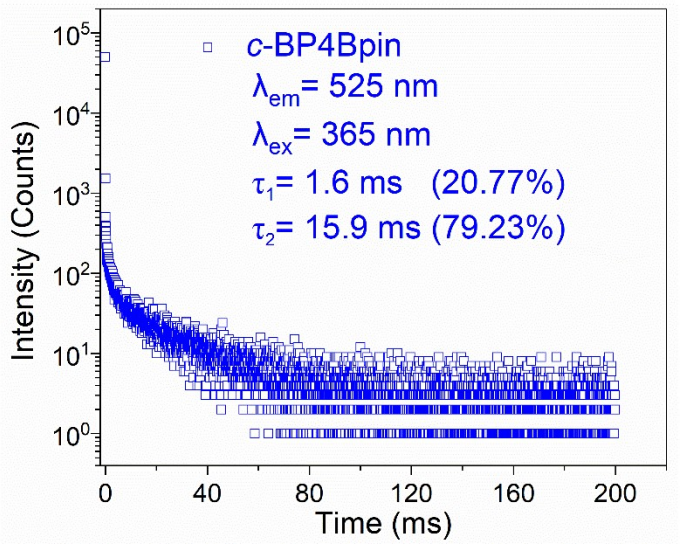

Figure S16 Time-resolved decay curves of crystalline *c*-BP4Bpin under 365 nm excitation at 300 K.

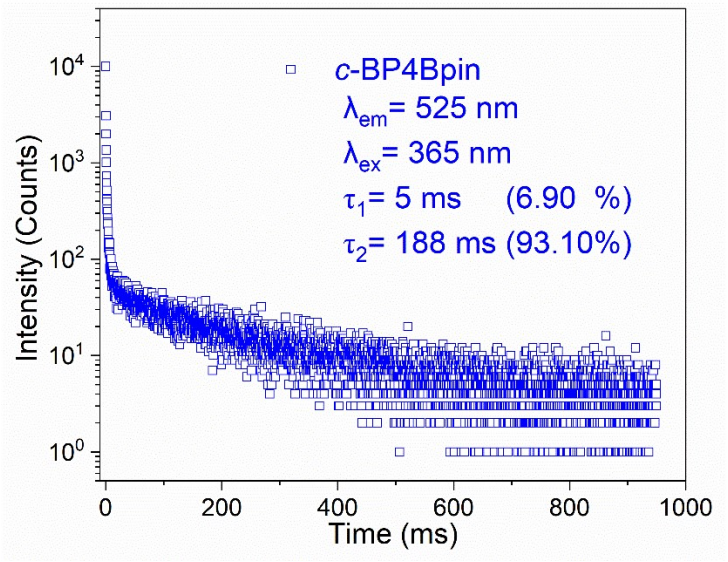

Figure S17 Time-resolved decay curves of crystalline *c*-BP4Bpin under 365 nm excitation at 77 K.

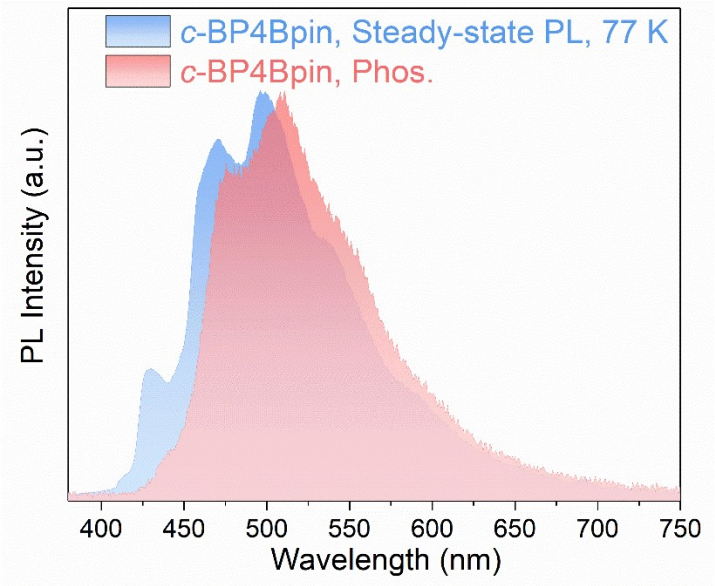

Figure S18 Steady-state PL (blue, λ_{ex} = 365 nm) and delayed spectra (red, delay 8 ms) of crystalline *c*-BP4Bpin at 77 K.

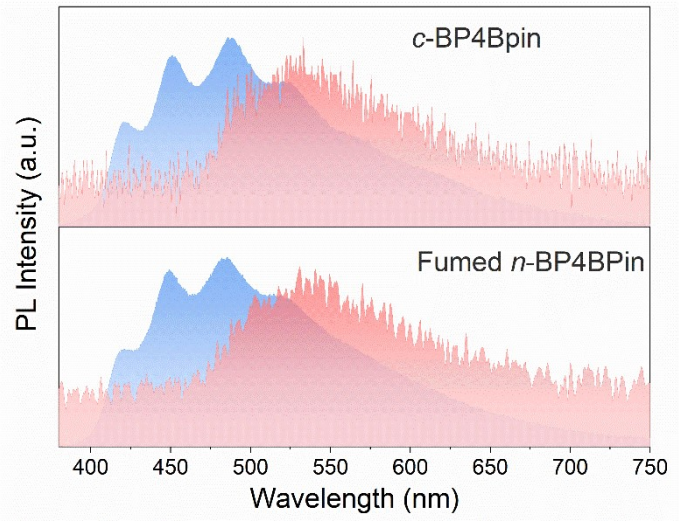

Figure S19 Steady-state PL (blue, λ_{ex} = 365 nm) and delayed spectra (red, delay 8 ms) of crystalline *c*-BP4Bpin and fumed *n*-BP4Bpin.

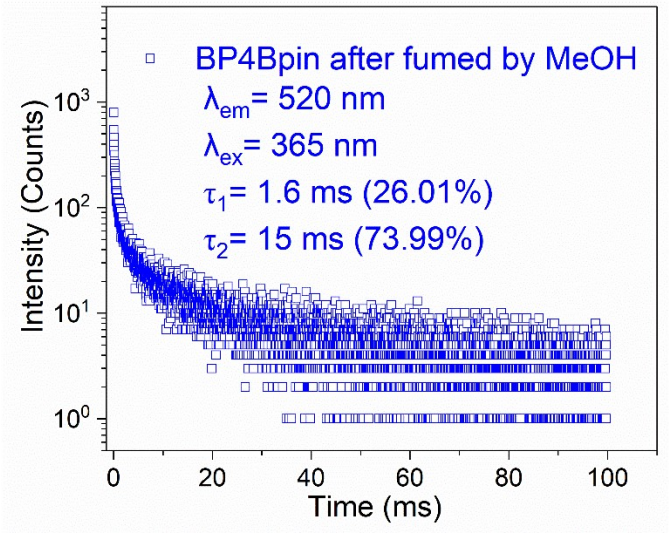

Figure S20 Time-resolved decay curves of crystalline BP4Bpin after fumed by MeOH under 365 nm excitation at 300 K.

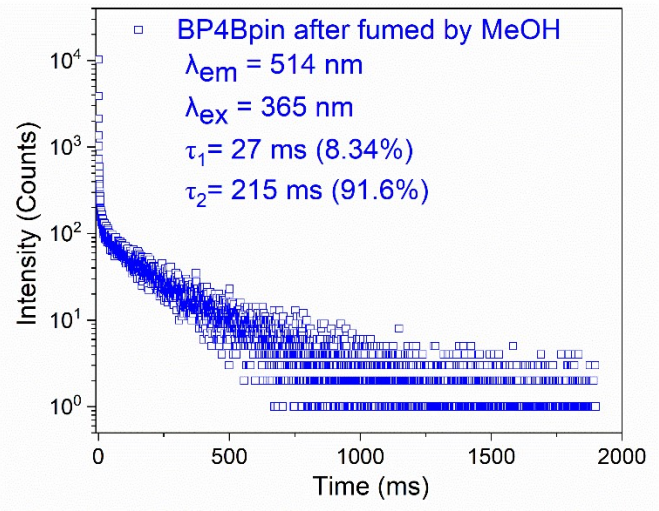

Figure S21 Time-resolved decay curves of crystalline BP4Bpin after fumed by MeOH under 365 nm excitation at 77 K.

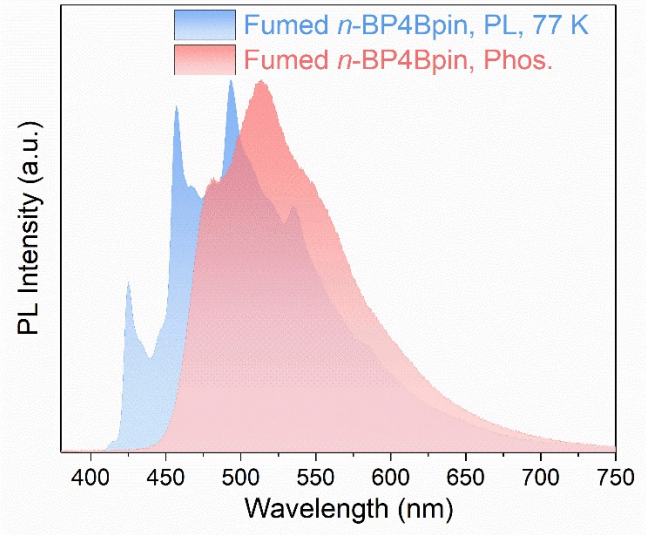

Figure S22 Steady-state PL (blue, λ_{ex} = 365 nm) and delayed spectra (red, delay 8 ms) of crystalline *n*-BP4Bpin after fumed by MeOH at 77 K.

Table S7 The CIE coordinates of crystalline *n*-BP4Bpin under UV irradiation at different temperature.

Temperature	**CIE *x***	**CIE *y***	**Peak**
25 ℃	0.3041	0.4989	528
30 ℃	0.3129	0.4808	528
35 ℃	0.3004	0.471	529
40 ℃	0.2989	0.4632	528
45 ℃	0.3002	0.4537	528
50 ℃	0.2905	0.432	493
55 ℃	0.2822	0.4168	493
60 ℃	0.2752	0.3883	493

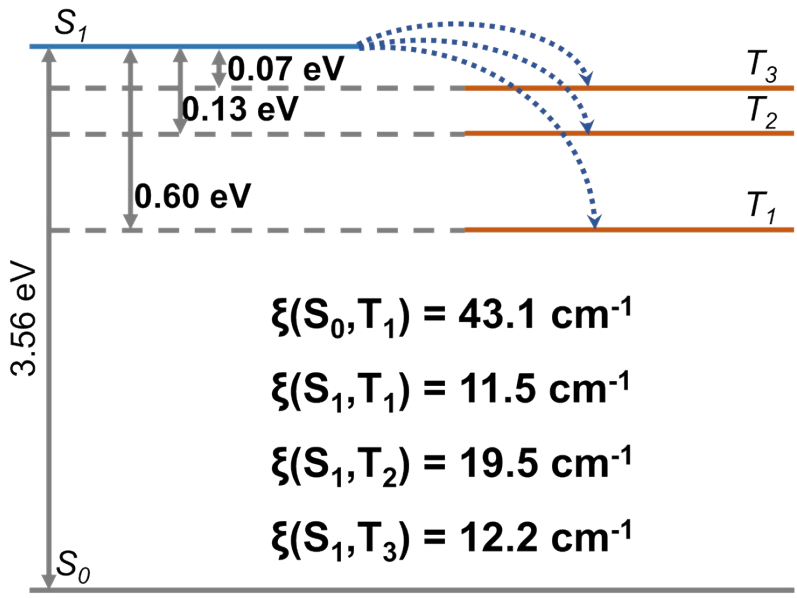

Figure S23 Theoretically-calculated energy levels and spin-orbit coupling constants between S_1 and lower-lying Tn with the corresponding single crystal structure of *c*-BP4Bpin.

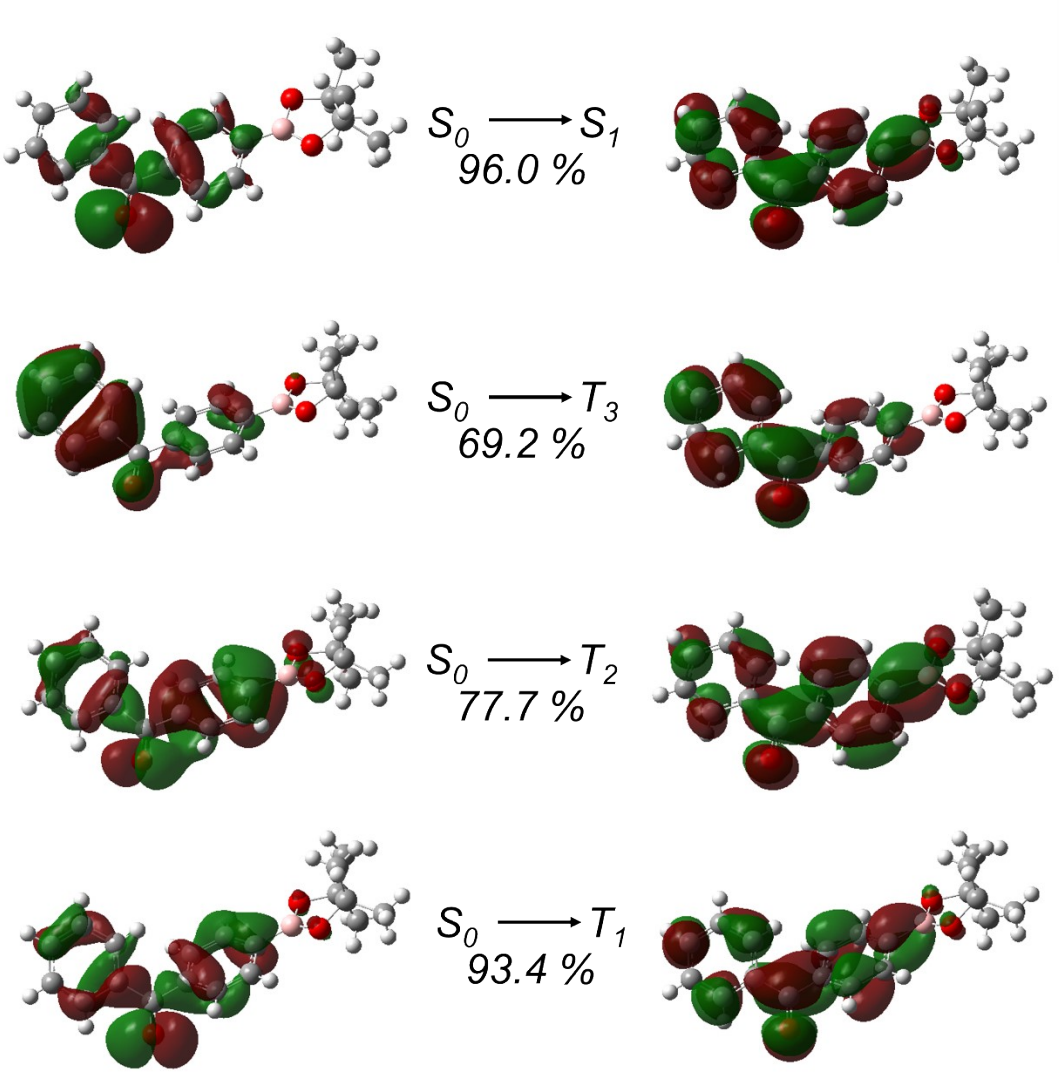

Figure S24 NTO distributions of S_1, lower-lying T_1, T_2 and T_3 at crystalline geometric structure of *n*-BP4Bpin.

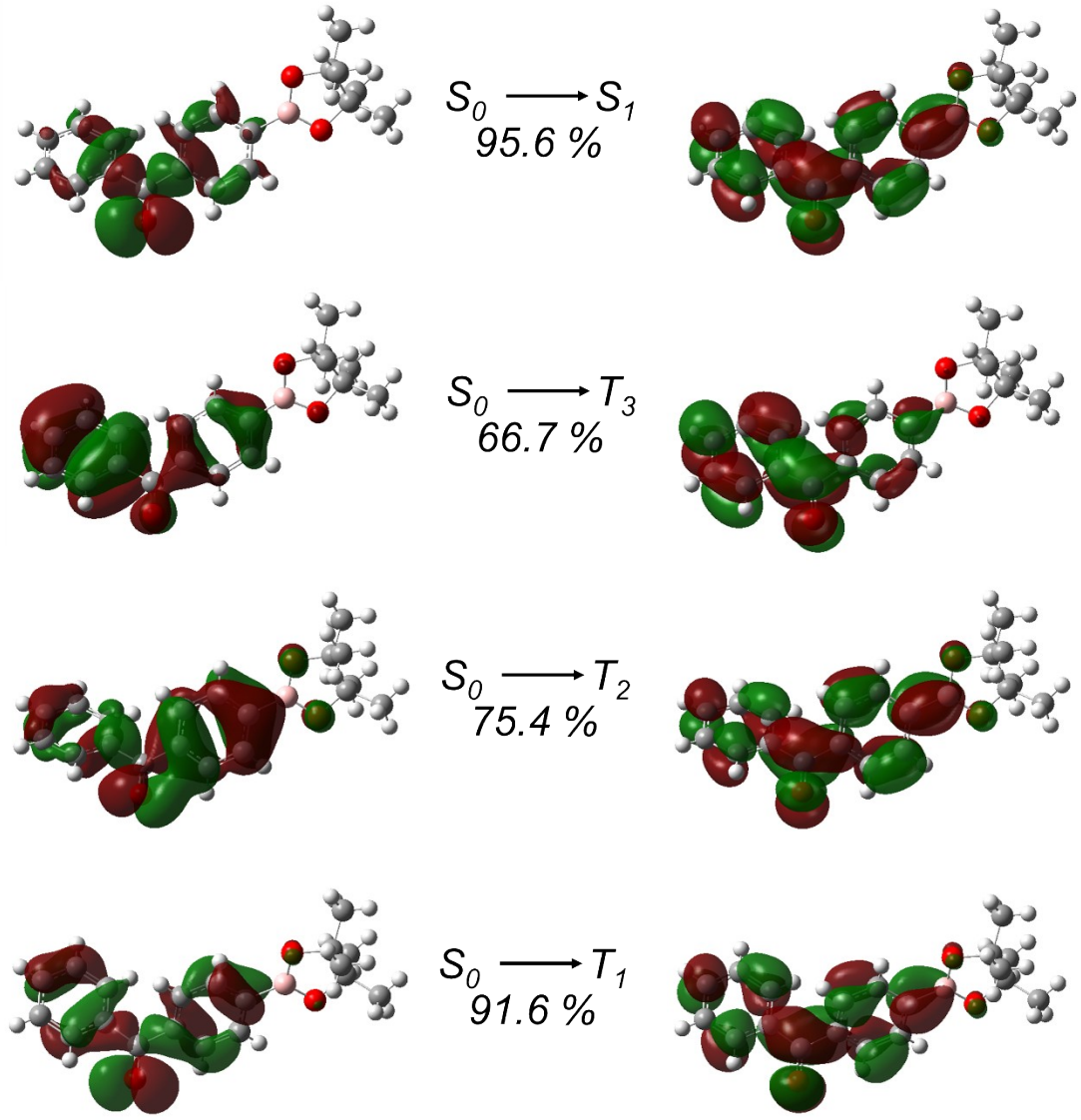

Figure S25 NTO distributions of S_1, lower-lying T_1, T_2 and T_3 at crystalline geometric structure of *c*-BP4Bpin.

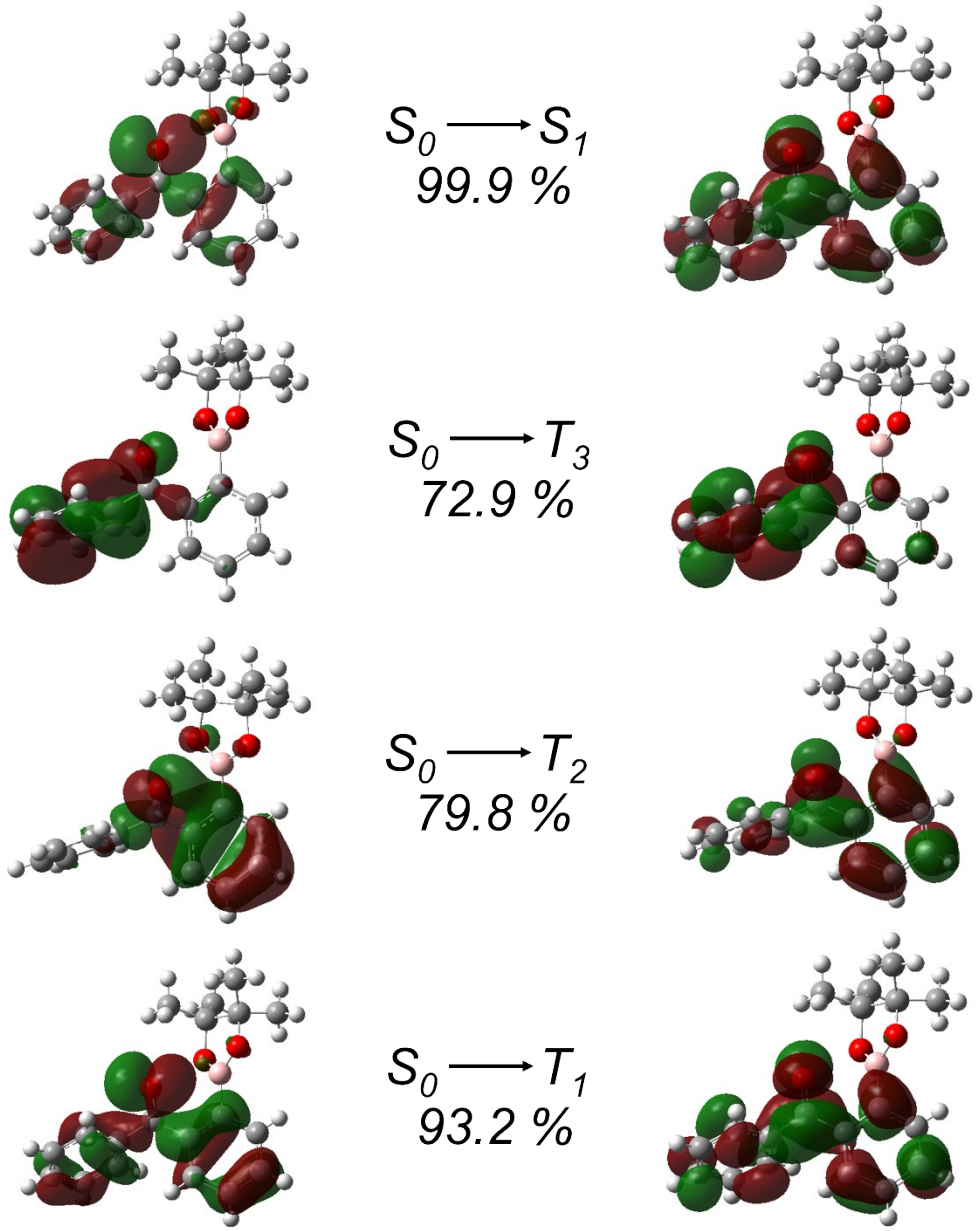

Figure S26 NTO distributions of S_1, lower-lying T_1, T_2 and T_3 at crystalline geometric structure of BP2Bpin.

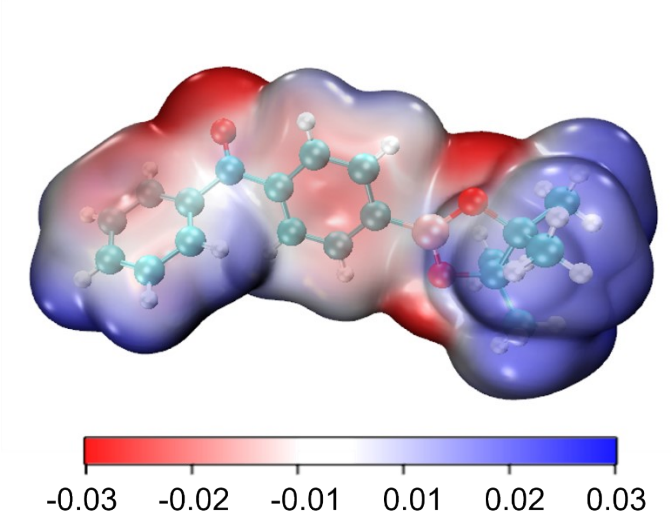

Figure S27 Electrostatic potential diagrams of *c*-BP4Bpin.

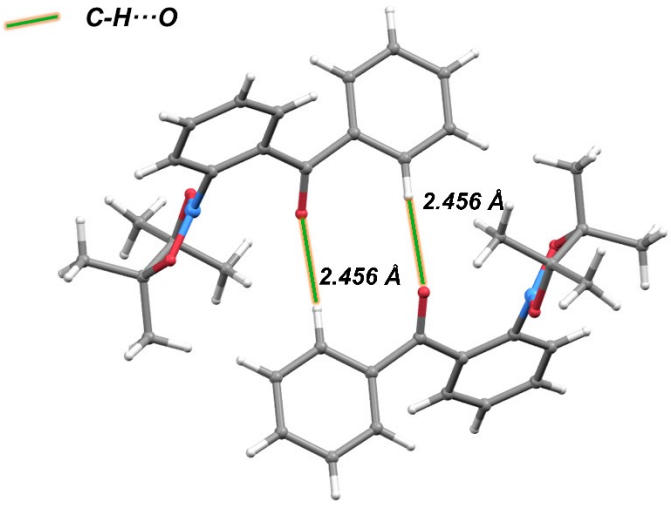

Figure S28 Single-crystal structures of BP2Bpin dimers (C-H···O intermolecular hydrogen bonds were shown).

References

1. A. D. Becke, *J. Chem. Phys.*, 1993, **98**, 5648-5652.
2. C. Lee, W. Yang and R. G. Parr, *Phys. Rev. B*, 1988, **37**, 785-789.
3. T. Lu and F. Chen, *J. Comput. Chem.*, 2012, **33**, 580-592.
4. E. R. Johnson, S. Keinan, P. Mori-SáNchez, J. Contreras-GarcíA, A. J. Cohen and W. Yang, *J. Am. Chem. Soc.*, 2010, **132**, 6498-6506.
5. C. Lefebvre, G. Rubez, H. Khartabil, J.-C. Boisson, J. Contreras-García and E. Hénon, *PCCP*, 2017, **19**, 17928-17936.
6. W. Humphrey, A. Dalke and K. Schulten, *J. Mol. Graph.*, 1996, **14**, 33-38.